3 September 1999

ELSEVIER

Chemical Physics Letters 310 (1999) 287–295

CHEMICAL PHYSICS LETTERS

www.elsevier.nl/locate/cplett

Distribution of single-molecule line widths

E. Barkai, R. Silbey *

Department of Chemistry and Center for Material Science and Engineering, Massachusetts Institute of Technology, Cambridge, MA 02139, USA

Received 25 May 1999; in final form 30 June 1999

Abstract

Single molecule spectroscopy shows that line shapes of guest molecules in low-temperature disordered solids vary from one molecule to the other. We consider a single molecule in a host lattice interacting with randomly distributed two level defects via a long range interaction. We investigate in detail the dipolar interaction and calculate the probability density of variances for high and low densities of defects. © 1999 Published by Elsevier Science B.V. All rights reserved.

1. Introduction

Modern experimental techniques have made it possible to perform time-dependent measurements of the optical spectrum of a single molecule embedded in a solid [1–5]. Using single-molecule spectroscopy (SMS), one may study many spectroscopic details obscured by inhomogeneous line broadening observed when the line shape of an ensemble of molecules is investigated. In disordered medium, each molecule is situated in a unique environment, hence the line shapes of single molecules are random functions. Fluctuation of energy, and hence line shapes, of a single molecules are believed to be induced by internal dynamics of randomly distributed defects, usually treated as two-level systems (TLS), which interact with the molecule via a long-range interaction [6–18].

Recent experiments [19–22] in glassy and defected crystalline materials have measured $h(\Delta\nu)$, the probability density of line widths of single molecules. These experiments show that $h(\Delta\nu)$ is asymmetrical and long-tailed. The line width $\Delta\nu$ is related to the line-shape variance W, according to $\Delta\nu = z\sqrt{W}$, and the dimensionless factor z depends on the line shape [16]. For non-crystalline media a continuum model [16,19,23] which assumes a dipole interaction shows that the probability density of W behaves like $g(W) \sim W^{-3/2}$ when $W \gg 1$ which implies that $h(\Delta\nu) = g(W)|\mathrm{d}W/\mathrm{d}\Delta\nu| \sim (\Delta\nu)^{-2}$. Currently, there is not sufficient experimental data to determine whether the continuum theory works quantitatively.

In this Letter, we consider a cubic lattice model for the distribution of variances W of single molecules in a disordered crystal. For dipole-like interaction, we show that **(a)** for high defect density $g(W)$ is well approximated by a sum of seven Gaussians reflecting the possible interactions with six nearest neighbors **(b)** for low defect density

* Corresponding author. Fax: +1-617-253-7030; e-mail: silbey@mit.edu

PII: S0009-2614(99)00797-6

$g(W)$ exhibits peaks separated by large gaps in which $g(W) \sim 0$ and this behavior replaces the $W^{-3/2}$ behavior of the continuum model. Thus, we show that the lattice structure has a rather strong influence on $g(W)$.

The distribution of variances can be analyzed in terms of uncorrelated random walks. This picture is due to the assumption of independent flipping events of the TLSs. The variance W can be written as a sum of independent contributions from TLSs

$$W = \sum_{i}^{N} w_i \tag{1}$$

where w_i is a contribution from the ith TLS in the system. As we show below, when the TLSs are distributed uniformly in space (i.e., the continuum model), the sum Eq. (1) can be analyzed in terms of the fundamental generalized central limit theorem [24–26]. Within the generalized central limit theorem, stable distributions replace the Gaussian distribution of the ordinary central limit theorem. Here we show that, in the continuum limit of our model, $g_{\mathrm{con}}(W)$ is an asymmetrical Lévy stable probability density with index γ determined by the interaction exponent and the dimensionality of the problem. For dipole-like interaction in three dimensions, $\gamma = 1/2$, our result for $g_{\mathrm{con}}(W)$ is identical to previous calculations on the dipolar interaction [16,23]. In recent years, stable distributions were shown to play an important role in diverse physical phenomena [27,28].

2. Model

We use a variant of the standard model for the interaction of a chromophore and a sea of defect TLSs. The molecule resides on the origin of a three-dimensional cubic lattice. The lattice spacing is unity. Each site is labeled with an index j. Site j (not including the origin) is described with an occupation parameter β_j, which can take the values 0 or 1, corresponding to the absence and presence of a fluctuating defect. The probability that lattice site j is occupied by such a defect is p. We assume that the occupancy of site j is independent of the occupancy of other lattice sites.

The defects are uncorrelated TLSs interacting with a chromophore by a long-range interaction. Every flip of a two-level system is assumed to shift the transition energy of the chromophore by the amount

$$\Delta E_j = \frac{\alpha \varepsilon_j}{|\boldsymbol{r}_j|^{\theta}}. \tag{2}$$

where α is a coupling constant, and $\boldsymbol{r}_j$ gives the location of the TLS on site j. ε_j are time-independent orientation parameters, taken to be $+1$ or -1 with equal probability. θ is an interaction exponent which for dipole interaction is $\theta = 3$. The total shift in energy of the chromophore is a sum of contributions from different defects

$$E(t) = \sum_{j} \alpha \frac{\beta_j \varepsilon_j \xi_j(t)}{|\boldsymbol{r}_j|^{\theta}}, \tag{3}$$

where $\xi_j(t)$ is a time-dependent occupation parameter taken to be 1 or 0, corresponding to the jth TLS being in its ground or excited state, respectively. We assume that all stochastic processes are independent and statistically identical. The time average $\overline{\left(\xi_i(t) - \overline{\xi_i(t)}\right)^2} \equiv \delta^2$ is given by standard thermal equilibrium occupation of the ground and first excited states of the identical TLSs [30].

The variance of the energy fluctuations is given by

$$W \equiv \frac{\left(\overline{E^2} - \overline{E}^2\right)}{\delta^2 \alpha^2} = \sum_{j} \frac{\beta_j}{|\boldsymbol{r}_j|^{2\theta}}, \tag{4}$$

where the sum is over all lattice sites. W in Eq. (4) will vary from one molecule to the other, depending on the environment in which each is situated. In this Letter, we investigate the statistical properties of the dimensionless random variable W.

Under certain conditions, W may model a linewidth [16,19]. The main assumptions being: (a) the measurement time is long as compared to the characteristic time between jumps in frequency space, (b) the line broadening due to coupling to phonon bath, laser intensity, and detection efficiency [29] is identical for all molecules, or very small, and (c) resonant lines do not split, i.e., weak coupling assumption.

One may limit the investigation of the model to $0 < p \leqslant 1/2$. For $p > 1/2$ one can redefine the problem where vacancies (i.e., empty lattice points) are considered as defects.

3. Continuum results

To contrast our lattice results, let us first consider the continuum version of our model. We consider the sum Eq. (1) with the number of TLSs $N \to \infty$ and the density of TLSs being $\rho = N/V$. The summands w_i are independent, identically distributed, random variables with a common probability density function $\eta(w)$. In terms of the random molecule TLS distance r_i, w_i in Eq. (1) is given by $w_i = 1/r_i^{2\theta}$. The probability density function $\eta(w)$ is related to the probability density of the random variables $\{r_i\}$, $\rho(r)$ according to $\eta(w) = |\mathrm{d}r/\mathrm{d}w|\,\rho(r)$. Using a uniform distribution of defects, in dimension D, $\rho(r)\,\mathrm{d}r\,\mathrm{d}\Omega = r^{D-1}\,\mathrm{d}r\,\mathrm{d}\Omega/V$ we find

$$\eta(w) \sim w^{-(1+\gamma)} \tag{5}$$

and $\gamma \equiv D/(2\theta)$, which means that when $\gamma < 1$ the first moment of the summand w_i diverges. Since the summands w_i are also independent and identically distributed, the generalized central limit theorem can be used to investigate the statistical properties of the sum Eq. (1). Most interesting interaction exponents satisfy $\theta > 3/2$; hence we shall limit ourselves to $\gamma < 1$. Using these assumptions, a short calculation shows that the characteristic function is

$$\langle \exp(\mathrm{i}k \cdot W) \rangle = \exp\left[-\rho A |k|^{\gamma} \left(1 - i \frac{k}{|k|} \tan(\gamma\pi/2) \right) \right] \tag{6}$$

where $A = \Gamma(1-\gamma)\cos(\gamma\pi/2) \int \mathrm{d}\Omega/D$. The characteristic function Eq. (6) is an asymmetrical Lévy stable characteristic function, its inverse Fourier transform $g_{\mathrm{con}}(W)$ is a stable Lévy probability density function behaving like $g_{\mathrm{con}}(W) \sim W^{-(1+\gamma)}$. Hence TLSs distributed randomly in a thin two-dimensional film interacting with the molecule via a dipole interaction, namely $\gamma = 1/3$, will exhibit a slower decay of $g_{\mathrm{con}}(W)$ as compared to similar TLSs in a three-dimensional system.

The analytical form of $g(W)$ is known for two cases. When $\gamma = 1/2$, corresponding to a three-dimensional system with dipole interaction $\theta = 3$,

$$g_{\mathrm{con}}(W) = \frac{1}{A^2} \frac{2}{\sqrt{\pi}} \left(\frac{2W}{A^2} \right)^{-3/2} \exp\left(-\frac{A^2}{2W} \right), \tag{7}$$

called Smirnov's density, and a second stable probability density with $\gamma = 1/3$ can be found in Ref. [31]. For $\gamma \neq 1/2, 1/3$ $g_{\mathrm{con}}(W)$ can be found using converging asymptotic expansions or tables [24–26,31]. Besides $\gamma = 1/3$ and $\gamma = 1/2$ also other types of interaction, responsible for inhomogeneous line broadening [32] may contribute to the probability density of variances W. Thus for multi-polar interactions we find $\gamma < 1/2$ while interaction with random electric fields or dislocation fields may lead to $\gamma > 1/2$.

According to Eq. (6), $\mathrm{d}/\mathrm{d}k[\langle \exp(\mathrm{i}k \cdot W) \rangle]\|_{k=0} = \infty$; hence in the continuum limit the averaged variance diverges. For dipole interaction, this is because, in the continuum model, the TLSs are allowed to be situated very close to the molecule on the origin. One may introduce a lower cutoff (in the lattice model this is the lattice spacing) and/or an upper cutoff (i.e., system size). Then the distribution of the variance would not be stable; however, for small (large) enough cutoff, one can still observe the characteristic $W^{-(1+\gamma)}$ decay with an upper cutoff for large W. Pfluegl et al. [16] calculated the explicit dependence of the distribution of variance on the lower cutoff for the case $\gamma = 1/2$.

4. Lattice model exact results

Let us investigate the lattice model. A disordered system is characterized by n_1 dipoles a distance $|\boldsymbol{r}_j|^2 = 1$ from the origin, n_2 dipoles a distance $|\boldsymbol{r}_j|^2 = 2$, etc. We define a disordered state with the sequence of numbers $\{n_1, n_2, \cdots, n_m\}$. m is an upper cutoff which gives the number of 'shells' we consider and the limit of $m \to \infty$ is of interest.

Let $\mathrm{Prob}(W = x)$ be the probability of finding a line width W equal to x. The characteristic function of $\mathrm{Prob}(W = x)$ is

$$\langle \exp(\mathrm{i}k \cdot W) \rangle = \prod_j \left[p \exp\left(\frac{\mathrm{i}k}{|\boldsymbol{r}_j|^{2\theta}} \right) + (1-p) \right], \tag{8}$$

the product $\prod_j$ is over all lattice points. Let $n_{|j|^2}^{\max}$ be the number of sites on the cubic lattice that are a

distance $|j|^2 = 1,2,3,\cdots$ from the origin. For example, for a three-dimensional system

$$n_1^{\max} = 6, n_2^{\max} = 12, n_3^{\max} = 8, n_4^{\max} = 6, n_5^{\max} = 24,$$

$$n_6^{\max} = 24, n_7^{\max} = 0, n_8^{\max} = 12,$$

$$n_9^{\max} = 30, n_{10}^{\max} = 24, n_{11}^{\max} = 24,$$

and from a standard continuum approximation $n_{|j|^2}^{\max} \sim 2\pi|j|$ for $|j| \gg 1$. We do not know of an explicit formula for $n_{|j|^2}^{\max}$ (for $D > 1$); however, these numbers can be easily calculated for large systems. One can use the lattice symmetry and the characteristic function Eq. (8) to obtain the solution for finite systems

$$\begin{aligned}\mathrm{Prob}(W = x) &= \sum_{n_1, n_2, \cdots, n_m | x} \binom{n_1^{\max}}{n_1}\binom{n_2^{\max}}{n_2}\cdots\binom{n_m^{\max}}{n_m} \\ &\quad \times p^{\sum_{i=1}^{m} n_i}(1-p)^{N - \sum_{i=1}^{m} n_i}, \end{aligned} \tag{9}$$

where $N = \sum_{i=1}^{m} n_i^{\max}$ is the number of lattice sites. In Eq. (9) $\sum_{n_1, n_2, \cdots, n_m | x}$ is a sum over all values of

$$\begin{aligned} n_1 &= 0, \cdots, n_1^{\max} \\ &\vdots \\ n_m &= 0, \cdots, n_m^{\max} \end{aligned} \tag{10}$$

which satisfy the condition

$$x = n_1 + n_2/2^{\theta} + \cdots n_m/m^{\theta}. \tag{11}$$

For $x \neq n_1 + n_2/2^{\theta} + \cdots n_m/m^{\theta}$ we have $\mathrm{Prob}(W = x) = 0$.

Eq. (11) describes the discrete spectrum of W of the lattice models which replaces the continuum spectrum of W of the continuum models.

The exact solution Eq. (9) can be evaluated with the aid of a computer for finite systems. Depending on θ, D and p, the convergence of the solution in the limit of large m may be rather slow. However, as we show in Section 5, at least for some choices of parameters, the exact solution can give useful information on the infinite lattice system.

5. Strong disorder

We limit our investigation to the case $D = 3$ and $\theta = 3$ (i.e., dipolar interaction).

To gain some insight into the meaning of Eq. (9), consider an approximate solution for $p = 1/2$. It is instructive to rewrite Eq. (9) as a sum of seven terms

$$\mathrm{Prob}(W = x) = \sum_{j_1 = 0}^{6} Q_{j_1} \mathrm{Prob}(W = x | n_1 = j_1), \tag{12}$$

where $\mathrm{Prob}(W = x | n_1 = j_1)$ is the conditional probability that $W = x$ when the number of occupied nearest-neighbor sites is equal j_1 and

$$Q_{j_1} = p^{j_1}(1-p)^{6-j_1}\binom{6}{j_1} \tag{13}$$

is the probability that j_1 nearest-neighbor sites are occupied. In Table 1, we show the cumulants of $\mathrm{Prob}(W = x | n_1 = j_1)$ obtained from the characteristic function. These cumulants are given in terms of $q = p - 1/2$ and the lattice sums

$$I(n) \equiv \sum_j \frac{1}{|\boldsymbol{r}_j|^{2n\theta}}, \tag{14}$$

where $n = 1,2\cdots$. For $D = 3, \theta = 3$, the converging sums $I(n)$ are evaluated using a computer without difficulty. In Table 2, we give the numerical values

Table 1
Cumulants of $\mathrm{Prob}(W = x | n_1 = j_1)$

n	κ_n
1	$j_1 + (1/2 + q)[I(1) - 6]$
2	$(1/4 - q^2)[I(2) - 6]$
3	$-2(1/4 - q^2)q[I(3) - 6]$
4	$(1/4 - q^2)(-1/2 + 6q^2)[I(4) - 6]$
5	$(1/4 - q^2)(4q - 24q^3)[I(5) - 6]$
6	$(1/4 - q^2)(1 - 30q^2 + 120q^4)[I(6) - 6]$
7	$(1/4 - q^2)(-17q + 240q^3 - 720q^5)$ $[I(7) - 6]$
8	$(1/4 - q^2)(-17/4 + 231q^2 - 2100q^4 + 5040q^6)$ $[I(8) - 6]$

Table 2
Numerical values of $I(n)$

n	1	2	3	4	5	6
$I(n)$	8.40184	6.20215	6.02388	6.00295	6.00037	6.00005

of $I(n)$; we see that $\lim_{n\to\infty} I(n) = 6$ which is the number of nearest neighbors on a $D = 3$ cubic lattice.

When $p = 1/2$, the cumulants in Table 1 show $\kappa_{2n+1} = 0$ and

$$3\kappa_2^2 \gg \kappa_4$$
$$15\kappa_2^3 \gg \kappa_6 + 15\kappa_4\kappa_2 . \qquad (15)$$

When these inequalities are satisfied, the conditional probability $P(W = x|j = n_1)$ behaves like the Gaussian distribution (i.e., the cumulants of the Gaussian vanish for $n > 2$). Our approximation is to replace $\mathrm{Prob}(W = x|n_1 = j_1)$ with a Gaussian with a variance and mean in accordance with the cumulants in Table 1. Therefore, let $g(W)\,\mathrm{d}W$ be the probability of finding the variance W in a small interval $(W, W + \mathrm{d}W)$, then

$$g(W) = \sum_{j_1=0}^{6} Q_{j_1} \frac{1}{\sqrt{2\pi\sigma_1^2}} \exp\left[-\frac{(W - j_1 - \upsilon)^2}{2\sigma_1^2}\right], \qquad (16)$$

where

$$\sigma_1^2 = \frac{[I(2) - 6]}{4} \qquad (17)$$

and

$$\upsilon = \frac{[I(1) - 6]}{2} . \qquad (18)$$

In Eq. (16), the sum over j_1 reflects the contribution from the six nearest-neighbor interactions while the finite width of the seven Gaussians reflects the interaction with the background.

The approximation $g(W)$ (in Eq. (16)) is a smooth continuous probability density function which replaces the exact expression for $g(W)$ (Eq. (9)) which

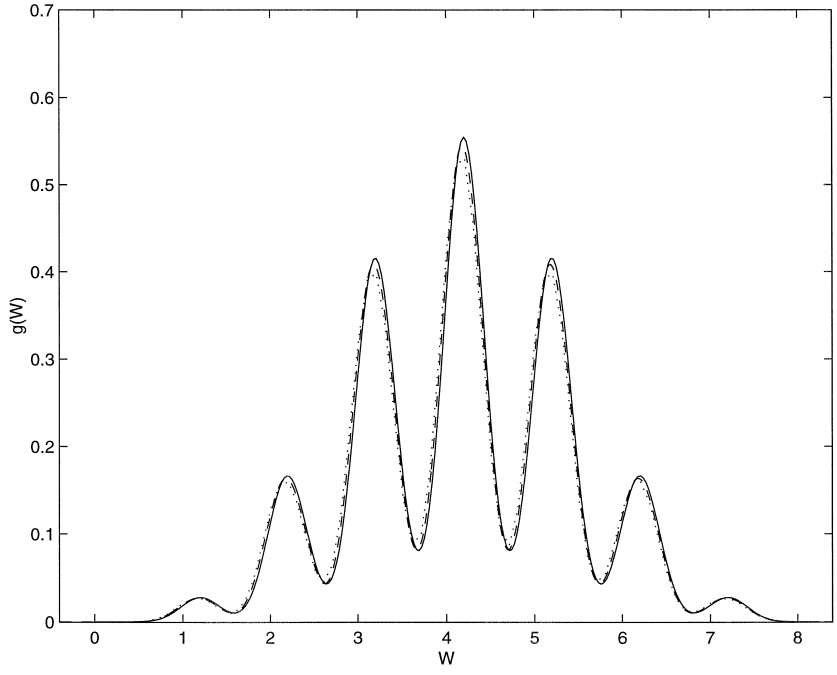

Fig. 1. The solid curve is $g(W)$ (Eq. (16)) exhibiting seven peaks which are due to the lattice structure. The dotted curve is a histogram (with a bin length 0.1) obtained with the exact result; the dashed curve is the solution obtained by a numerical Fourier inversion of the characteristic function (Eq. (8)).

is a sum of closely spaced delta functions. To make a comparison between the exact and approximate solutions, we have built a histogram based on the exact solution. This histogram is shown in Fig. 1 together with the approximation Eq. (16). The exact result was derived for a finite system, with $m = 8$, for which the solution has not yet reached its thermodynamic ($m \to \infty$) limit. To overcome this, we noice that the axis of symmetry of the exact solution is $I(1)/2$. Hence we (slightly) shift the exact finite size solution, in such a way that the axis of symmetry of $g(W)$ is on $I(1)/2$. Also shown in Fig. 1 is $g(W)$ obtained by a numerical inversion of the characteristic function (Eq. (8)). The approximate solution (Eq. (16)), the exact solution based on Eq. (9) and the numerical Fourier transform (all presented in Fig. 1) are in good agreement.

6. Weak disorder

What is the relation between the solution of the continuum and lattice models? One might anticipate that for low defect density, $p \ll 1$, the dipoles situated far away from the molecule play an important role and then the lattice structure is of lesser importance. We rewrite the characteristic function Eq. (8) as

$$\langle \exp(\mathrm{i}k \cdot W) \rangle = \exp\left\{ \sum_j \ln\left[1 + p\left(\mathrm{e}^{\mathrm{i}k/|j|^6} - 1\right)\right] \right\}, \tag{19}$$

and expand the logarithm to obtain

$$\langle \exp(\mathrm{i}k \cdot W) \rangle = \exp\left[-p \sum_j \left(1 - \mathrm{e}^{\mathrm{i}k/|j|^6}\right) \right] \tag{20}$$

for $p \ll 1$. Converting the sum in Eq. (20) into an integral we find

$$\langle \exp(\mathrm{i}k \cdot W) \rangle_{\mathrm{con}} = \exp\left[-p 4\pi/3 \int_{r_c}^{\infty} \mathrm{d}r^3 \left(1 - \mathrm{e}^{\mathrm{i}k/|r|^6}\right) \right] \tag{21}$$

where r_c is a low cutoff and the subscript indicates that we are considering a continuum model. Taking the limit $r_c \to 0$ in Eq. (21), we obtain the stable characteristic function Eq. (6). For the lattice model the lattice spacing $a = 1$ is a lower cutoff, we have checked that for $r_c \simeq 1$ the continuum probability density function with and without a cutoff are practically identical.

In Fig. 2 we show $g(W)$, obtained using a numerical Fourier transform of the exact solution Eq. (19). We observe satellite peaks due to the lattice structure. These peaks are separated by large gaps in which $g(W) \simeq 0$. While $g(W)$ is mostly concentrated in a small region close to the origin (say $W < 0.01$), corresponding to interaction with distant defects, rare events with very large variance W are predicted to be significant.

Also shown in Fig. 2 are the stable Smirnov density Eq. (7) and the numerical Fourier transform of the characteristic function with finite cutoff r_c in Eq. (21). We find qualitative agreement between the lattice and continuum models, but only for small W. The deviation of the lattice solution from the continuum solution is most significant in the large W tail of $g(W)$ where the continuum model predicts a $W^{-3/2}$ power law decay. This behavior can be easily understood. A molecule whose variance W is large implies that some lattice points close to the origin are occupied by defects. For the defects close to the origin we can hardly expect a continuum model to work well.

Since the continuum approximation does not work well we develop qualitative approximation valid for small p which explains the the origin of the satellite peaks shown in Fig. 2. Our approach is similar to that sketched by Stoneham (see Section 5.2 in Ref. [32]) and used by Orth et al. [33] in the context of inhomogeneous line broadening. We divide the crystal into two regions. Within the first spherical inner region, which we call region 1, the lattice is treated as discrete and the rest of the crystal, region 2, is treated as a continuum. The radius of the inner region is $\sqrt{l}$ and l is an integer. The exact solution is written as

$$\mathrm{Prob}(W = x) = \sum_{j_1, \cdots, j_l} Q_{j_1, \cdots, j_l} \mathrm{Prob}(W = x | n_1 = j_1, \cdots, n_l = j_l) \tag{22}$$

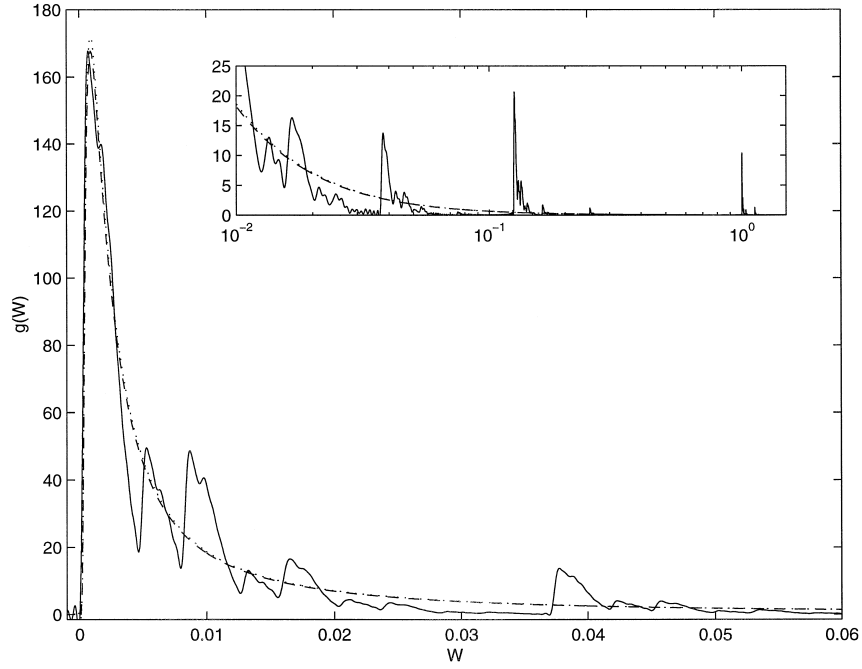

Fig. 2. The solid curve is $g(W)$ for the case $p = 0.01$, obtained by a numerical Fourier transform of the lattice characteristic function. The dashed curve is Smirnov's stable probability density function, and the dotted curve is the continuum solution with a finite cutoff $r_c = 1$. On the scale of the plot, the two continuum solutions are indistinguishable. In the inset, we show the tail of $g(W)$ on a semi-log plot.

with

$$Q_{j_1,\cdots,j_l} = (1-p)^{N-\sum_{i=0}^{l} j_i} p^{\sum_{i=0}^{l} j_i} \binom{6}{j_1} \cdots \binom{n_l^{\max}}{j_l}, \tag{23}$$

and $N = \sum_{i=1}^{l} n_i^{\max}$. $Q_{j_1,\cdots,j_l}$ is the probability that $n_1 = j_1$, $n_2 = j_2$, etc., and $\mathrm{Prob}(W = x | n_1 = j_1, n_2 = j_2 \cdots)$ in Eq. (22) is the probability that $W = x$ subject to the condition that the number of n_1 sites is j_1, etc.

Our approximation, valid for $p \ll 1$, involves two steps; first, we replace the conditional probabilities $\mathrm{Prob}(W = x | n_1 = j_1, \cdots, n_l = j_l)$ with smooth normalized non-negative probability densities and then truncate the sum Eq. (22). The integer l in Eq. (22) divides the system into two and the limit of large l must be considered. Practically, we increase l until our results converge. As in Section 5, we replace the discrete $\mathrm{Prob}(W = x)$ with the continuum probability density function $g(W)$.

The first step is to replace the conditional probability $\mathrm{Prob}(W = x | n_1 = j_1, \cdots, n_l = j_l)$, in Eq. (22), with its continuum approximation. For this aim we use the conditioned characteristic function

$$\langle \exp(\mathrm{i}k \cdot W) \rangle_{n_1 = j_1, \cdots, n_l = j_l} = \mathrm{e}^{\mathrm{i}k x_{\min}} \left\{ \prod_{j \neq j_1, \cdots, j_l} \left[p \exp\left(\mathrm{i}k/|\boldsymbol{r}_j|^6\right) + (1-p) \right] \right\}, \tag{24}$$

where the multiplication is over all lattice points excluding those in region 1 and $x_{\min} = \sum_{i=1}^{l} j_i / i^3$. We now use the same procedure given in Eqs. (19) and (20), and then $\mathrm{Prob}(W = x | n_1 = j_1, \cdots, n_l = j_l)$ in Eq. (22) is replaced with

$$g_{j_1,\cdots,j_l}(W) = \begin{cases} Sm(r_c, W - x_{\min}) & \text{if } W > x_{\min} \\ 0 & \text{if } W < x_{\min}, \end{cases} \tag{25}$$

where $Sm(r_c, W)$ is the inverse Fourier transform of the continuum characteristic function Eq. (21) found numerically. In Eq. (25) $r_c = \sqrt{l}$ is the low cutoff reflecting the fact that we are treating region 2 as a continuum. The main assumption that we are using is

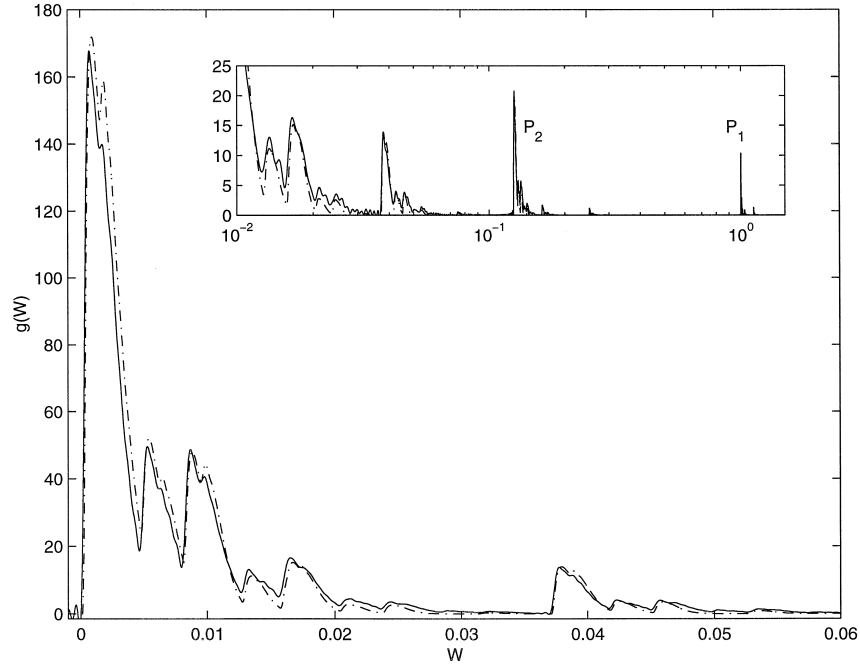

Fig. 3. The same as Fig. 2 with the approximate solution (Eq. (26)) added as a dot–dashed line. To obtain the approximate result, we used $l = 9$.

that when l is large enough the exact lattice sums may be replaced with the appropriate integrals.

For large l the summation in Eq. (22) is formidable, for example if $l = 9$ the sum is over e^{21} states. However since $p \ll 1$ we may use a second approximation and truncate the sum in Eq. (22). The lowest order of approximation is to consider only the term proportional to $Q_{0,0,\cdots,0}$ and this term gives the contribution from an empty region 1. The first-order corrections, are l terms in Eq. (22) proportional to $Q_{1,0,0,0,\cdots}$, $Q_{0,1,0,0,\cdots}$, etc. These terms imply that a single defect is residing in region 1. The $l(l+1)/2$ second-order terms are $Q_{1,1,0,0,\cdots}$, $Q_{1,1,0,0,\cdots}$, etc., and $Q_{2,0,\cdots}$, $Q_{0,2,\cdots}$, etc. We therefore have

$$g(W) = Q_{0,\cdots,0}\, g_{0,\cdots,0}(W) + \sum_{j_1+j_2+\cdots j_l=1} Q_{j_1,\cdots,j_l}\, g_{j_1,\cdots,j_l}(W) + \sum_{j_1+j_2+\cdots j_l=2} Q_{j_1,\cdots,j_l}\, g_{j_1,\cdots,j_l}(W) + \cdots \tag{26}$$

where the summation $\sum_{j_1+j_2+\cdots j_l=1}$ is over all values of $j_1 \geq 0, j_2 \geq 0 \cdots$ which satisfy the condition $j_1 + j_2 + \cdots j_l = 1$.

The probability that region 1 is empty for finite p goes to zero for very large l, and then the truncation procedure is not valid. Our approximation will work well only if l is large; however, p is small enough to ensure that the truncated sum Eq. (26) is approximately normalized to unity. For a given p and l this can be easily checked, since the functions $Sm(r_c, W - x_{\min})$ in Eq. (26) are normalized probability densities.

Fig. 3 shows the approximate solution Eq. (26) together with the results obtained using numerical Fourier transform of the characteristic function Eq. (19), for the case $p = 0.01$. The approximation was calculated using the first- and second-order correction terms in Eq. (26). Good agreement between the numerical and approximate result is found. Each peak we observe in Fig. 3 can be related to a microscopic configuration of defects within region 1. For example the peaks labeled P_1 (P_2) in Fig. 3, correspond to a defect situated on one of the

nearest-neighbor (next to nearest neighbors) sites, respectively.

7. Summary

We have studied the distribution of variances of single molecules interacting with TLSs distributed randomly on a lattice. Due to the power law interaction of the TLSs with the molecules the continuum version of our model can be analyzed using the generalized central limit. When the density of defects is high, $p = 1/2$, and when the interaction is dipolar, the probability density $g(W)$, exhibits seven distinct Gaussian peaks due to possible interactions with defects on six nearest-neighbor lattice sites. When the density of defects is low, several non-symmetrical peaks are observed. Large gaps in which $g(W) \sim 0$ separate these peaks. A simple theory was used to explain this behavior. For this case the peaks correspond to a single defect located on discrete distances from the molecule. Thus our results show that the distribution of variances and hence also the distribution of line widths are very sensitive to the lattice structure.

Acknowledgements

The research was supported in part by a grant from the NSF.

References

[1] T. Bache, W.E. Moerner, M. Orrit, U.P. Wild (Eds.), Single-Molecule Optical Detection, Imaging and Spectroscopy VCH, 1996.
[2] S. Nie, R.N. Zare, Ann. Rev. Biophys. Biomol. Struct. 26 (1997) 567.
[3] T. Plathotnik, E. Donley, U.P. Wild, Ann. Rev. Phys. Chem. 48 (1997) 181.
[4] X.S. Xie, J.K. Trautman, Ann. Rev. Phys. Chem. 49 (1998) 441.
[5] W.E. Moerner, M. Orrit, Science 283 (1999) 5408.
[6] L. Narasimhan, K. Littau, D. Pack, Y. Bai, A. Elschner, M. Fayer, Chem. Rev. 90 (1990) 439.
[7] P.D. Reilly, J.L. Skinner, Phys. Rev. Lett. 71 (1993) 4257.
[8] A. Suarez, R. Silbey, Chem. Phys. Lett. 218 (1994) 445.
[9] A. Suarez, R. Silbey, J. Phys. Chem. 98 (1994) 7329.
[10] P.D. Reilly, J.L. Skinner, J. Chem. Phys. 101 (1994) 959.
[11] P.D. Reilly, J.L. Skinner, J. Chem. Phys. 101 (1994) 965.
[12] G. Zumofen, J. Klafter, Chem. Phys. Lett. 219 (1994) 303.
[13] Y. Tanimura, H. Takano, J. Klafter, J. Chem. Phys. 108 (1998) 1851.
[14] E. Geva, J.L. Skinner, J. Phys. Chem. B 101 (1997) 8920.
[15] F.L.H. Brown, R.J. Silbey, J. Chem. Phys. 108 (1998) 7434.
[16] W. Pfluegl, F.L.H. Brown, R.J. Silbey, J. Chem. Phys. 108 (1998) 6876.
[17] E. Geva, J.L. Skinner, Chem. Phys. Lett. 287 (1998) 125.
[18] Y. Zhao, V. Chernyak, S. Mukamel, J. Phys. Chem. A 102 (1998) 6614.
[19] L. Fleury, A. Zumbusch, M. Orrit, R. Brown, J. Bernard, J. Luminesc. 56 (1993) 15.
[20] J. Tittel, R. Kettner, Th. Basche, C. Brauchle, H. Quante, K. Mullen, J. Luminesc. 64 (1995) 1.
[21] M. Vacha, Y. Liv, H. Nakatsuka, T. Tani, J. Chem. Phys. 106 (1997) 8324.
[22] B. Kozankiewicz, J. Bernard, M.J.J. Orrit, Chem. Phys. 101 (1994) 9377.
[23] L. Fleury, Ph.D. thesis, University of Bordeaux, 1995.
[24] P. Lévy, Théorie de l'addition des variables aléatories, Gauthier–Villars, Paris, 1937.
[25] B.V. Gnedenko, A.N. Kolmogorov, Limit Distributions for Sums of Independent Random Variables, Addison–Wesley, Reading, MA, 1954.
[26] W. Feller, An Introduction to Probability Theory and Its Applications, vol. 2, Wiley, 1970.
[27] B. Mandelbrot, The Fractal Geometry of Nature, Freeman, San Francisco, CA, 1982.
[28] J. Klafter, M.F. Shlesinger, G. Zumofen, Phys. Today 49 (1996) 33.
[29] L. Kador, J. Phys. Chem. A 102 (1998) 9745.
[30] That is, we assume that all defects flip many times within the experimental time scale to make the thermal equilibrium assumption correct. We note that in other situations δ may be time dependent. This does not alter the conclusions we reach in this Letter.
[31] E.W. Montroll, J.T. Bendler, J. Stat. Phys. 34 (1984) 129.
[32] A.M. Stoneham, Rev. Mod. Phys. 41 (1969) 82.
[33] D.L. Orth, R.J. Mashl, J.L. Skinner, J. Phys.: Condens. Matter 5 (1993) 2533.